Magnetic Order in the Pseudogap Phase of High-T_C Superconductors

B. Fauqué,[1] Y. Sidis,[1] V. Hinkov,[2] S. Pailhès,[1,3] C. T. Lin,[2] X. Chaud,[4] and P. Bourges[1,*]

[1]*Laboratoire Léon Brillouin, CEA-CNRS, CEA-Saclay, 91191 Gif sur Yvette, France*
[2]*MPI für Festkörperforschung, Heisenbergstrasse 1, 70569 Stuttgart, Germany*
[3]*LNS, ETH Zurich and Paul Scherrer Institute, CH-5232 Villigen PSI, Switzerland*
[4]*CRETA/CNRS, 25 Avenue des Martyrs, BP 166, 38042 Grenoble cedex 9, France*

(Received 18 October 2005; published 15 May 2006)

One of the leading issues in high-T_C superconductors is the origin of the pseudogap phase in underdoped cuprates. Using polarized elastic neutron diffraction, we identify a novel magnetic order in the $YBa_2Cu_3O_{6+x}$ system. The observed magnetic order preserves translational symmetry of the lattice as proposed for orbital moments in the circulating current theory of the pseudogap state. To date, it is the first direct evidence of a hidden order parameter characterizing the pseudogap phase in high-T_C cuprates.

DOI: 10.1103/PhysRevLett.96.197001 PACS numbers: 74.72.−h, 74.25.Dw, 74.25.Ha, 75.25.+z

In optimally and underdoped regimes, high-T_C copper oxide superconductors exhibit a pseudogap state [1–4] with anomalous magnetic [5], transport [6], thermodynamic [7], and optical [3] properties below a temperature, T^*, large compared to the superconducting (SC) transition temperature, T_c. The origin of the pseudogap is a challenging issue as it might eventually lead to identify the superconducting mechanism [1]. Two major classes of theoretical models attempt to describe the pseudogap state: In the first case, it represents a precursor of the superconducting d-wave gap [8,9] with preformed pairs below T^* which would acquire phase coherence below T_c [9,10]. In the second approach, the pseudogap is associated with either an ordered [11–16] or a disordered phase [1,17,18] competing with the SC one. The order parameter associated with these competing phases may involve charge and spin density waves [14–16] or charge currents flowing around the CuO_2 square lattice, such as D-charge density wave [13] or orbital circulating currents (CCs) [11,12].

Most of these phases break the translation symmetry of the lattice (TSL). Therefore, they may induce charge, nuclear, or magnetic superstructures that can be probed by neutron or x-ray diffraction techniques. In contrast, CC phases [11,12] preserve the TSL as they correspond to 4 or 2 current loops per unit cell (referred as Θ_I and Θ_{II} phases, respectively). These charge currents could be identified by virtue of the pattern of ordered orbital magnetic moments pointing perpendicularly to the CuO_2 planes. These orbital magnetic moments should be detectable by neutron diffraction. Although the TSL is preserved, the magnetic signature of the CC phase does not reduce to ferromagnetism: the loops are staggered within each unit cell corresponding to a zero magnetic propagation wave vector, $\mathbf{Q} = 0$, but with no net magnetization. In neutron diffraction, the magnetic intensity superimposes on the nuclear Bragg peak, meaning that these experiments are very delicate as the magnetic intensity $\propto M^2$ (M is the magnetic moment) is expected to be very small as compared to the nuclear Bragg peaks. In order to detect this hidden magnetic response, polarized neutron experiments [19,20] which allow one to separate magnetic and nuclear cross sections are then required.

As proposed by Varma [11,12], there are two possible CC phases preserving TSL. The first (the phase Θ_I) has not been detected by polarized elastic neutron scattering experiments [20]. Although it is controversial, a recent angle-resolved photoemission spectroscopy measurement observed a dichroic signal in the $Bi_2Sr_2CaCu_2O_{8+\delta}$ system consistent with the phase Θ_{II} [21]. Here, we have performed polarized elastic neutron scattering experiments to test the magnetic moments of this second CC state which actually had never been attempted before. We successfully report the first signature of a novel magnetic order in the pseudogap state of $YBa_2Cu_3O_{6+x}$ (YBCO). The pattern of the observed magnetic scattering corresponds to the one expected in the circulating current theory of the pseudogap state with two current loops per CuO_2 unit cell, phase Θ_{II} [11,12]. Alternatively, a decoration of the unit cell with staggered moments on the oxygen sites could also account for the measurements.

All the polarized neutron diffraction measurements were collected on the 4F1 triple-axis spectrometer at the Laboratoire Léon Brillouin, Saclay, France. Our polarized neutron diffraction setup is similar to that originally described in [19] with a polarized incident neutron beam at $E_i = 14.7$ meV obtained with a polarizing supermirror (bender) and with an Heusler analyzer (see also Refs. [20,22] in the context of high-T_C cuprates). The direction of the neutron spin polarization, $\mathbf{P}$, at the sample position is selected by a small guide field $\mathbf{H}$ of the order of 10 G [23]. Using that configuration, we monitor for each measured point the neutron scattering intensity in the spin-flip (SF) channel, where the magnetic intensity $\propto M^2$ is expected, and in the non-spin-flip (NSF) channel which measures the nuclear scattering. To have similar counting statistics on both SF and NSF, we count the SF channel systematically 20 times longer than the NSF. We define the normalized SF intensity as $I_{\text{norm}} = I_{\text{SF}}/I_{\text{NSF}}$ [inverse of the

flipping ratio (FR)]. With that setup, a typical flipping ratio, ranging between 40 and 60, is obtained. However, even with that high FR, the SF intensity is mainly coming from the NSF nuclear Bragg peak through unavoidable polarization leakage (corresponding to about ~90%–95% of the SF intensity). As a very stable and homogeneous neutron polarization is essential through the data acquisition, all the data have been obtained in a continuous run versus temperature. We prove that method to be efficient enough to see weak magnetic moments ($\sim 0.05 \mu_B$) on top of nuclear Bragg peaks; see, e.g., the first determination of the *A*-type antiferromagnetism in Na cobaltate systems [24].

We quote the scattering wave vector as $\mathbf{Q} = H\,\mathbf{a}^* + K\mathbf{b}^* + L\mathbf{c}^* \equiv (H, K, L)$ in units of the reciprocal lattice vectors, $\mathbf{a}^* \sim \mathbf{b}^* = 1.63$ Å^{-1} and $\mathbf{c}^* = 0.53$ Å^{-1}. Most of the data have been obtained in a scattering plane where all Bragg peaks like $\mathbf{Q} = (0, K, L)$ were accessible [in twinned samples, this is indistinguishable from Bragg peaks with $\mathbf{Q} = (H, 0, L)$]. In order to reveal small magnetic moments, measurements have been performed on the weakest nuclear Bragg peaks having the proper symmetry for the CC phase [25] [the Bragg peak $\mathbf{Q} = (0, 1, 1)$ offers the best compromise].

We have studied five different samples (see Table I): four samples in the underdoped regime and one in the overdoped regime. In Fig. 1(a), we report the raw neutron intensity measured at $\mathbf{Q} = (0, 1, 1)$ for the SF channel and for the NSF channel for an underdoped sample $YBa_2Cu_3O_{6.6}$(d) (sample C). The measurement has been done with a neutron polarization $\mathbf{P} \parallel \mathbf{Q}$ [see Fig. 1(b)] where the magnetic scattering is entirely spin flip [19,20,22,23]. Between room temperature and a temperature $T_{\mathrm{mag}} \simeq 220$ K, the NSF and SF intensities display the same temperature variation within error bars. Then, for $T < T_{\mathrm{mag}}$, the NSF is essentially flat, whereas the SF intensity increases noticeably at low temperature. This behavior signals the presence of a spontaneous magnetic order below T_{mag} on top of the nuclear Bragg peaks. In Fig. 1(c), we show the normalized magnetic intensity as a function of the temperature for the four underdoped samples and the overdoped sample. For the four underdoped samples, the magnetic intensity increases at low temperature below a certain temperature T_{mag}, whereas no magnetic signal is observed in the Ca-YBCO overdoped sample (sample E).

We perform further measurements where the neutron polarization is along the complementary directions, as shown in Fig. 1(b), either the vertical direction $\mathbf{P} \parallel \mathbf{z}$ or $\mathbf{P} \perp \mathbf{Q}$ but still within the horizontal scattering plane. The observance of the polarization selection rule for a magnetic signal, $I_{\mathbf{P}\parallel\mathbf{Q}} = I_{\mathbf{P}\parallel\mathbf{z}} + I_{\mathbf{P}\perp\mathbf{Q}}$, in the three polarizations, as

TABLE I. List of samples utilized in the polarized elastic neutron experiments. The experiments were performed in the (Y, Ca)$Ba_2Cu_3O_{6+x}$ family for five samples from the underdoped (ud) to overdoped (ov) part of the cuprates phase diagram. (t) and (d) stand for twinned and detwinned samples, respectively. References are given where the samples have been described in previous neutron scattering studies.

Sample	x	$T_{c,\mathrm{onset}}$ (K)	T_{mag} (K)	References
A	$O_{6.5}$(t)	ud 54	300 ± 10	[22]
B	$O_{6.6}$(t)	ud 61	250 ± 20	[26]
C	$O_{6.6}$(d)	ud 64	220 ± 20	[27]
D	$O_{6.75}$(t)	ud 78	170 ± 30	···
E	Ca(15%) − $O_{7-\delta}$(t)	ov 75	≃ 0	[28]

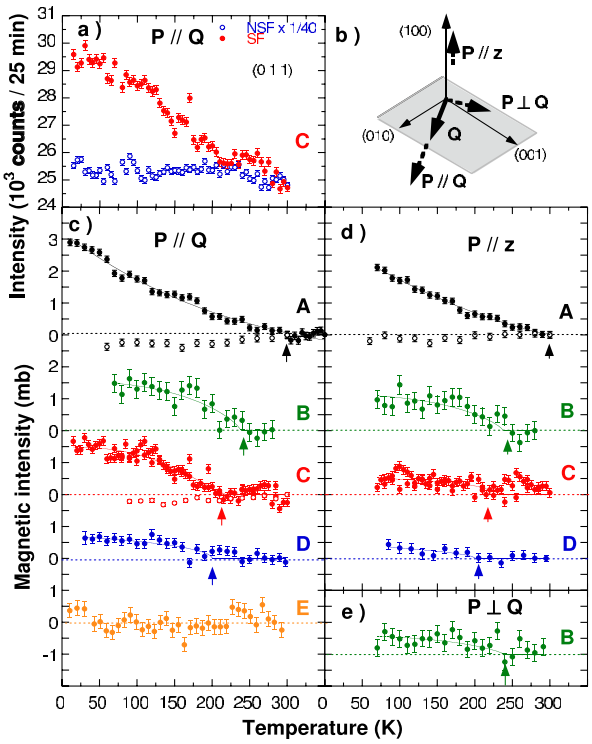

FIG. 1 (color online). (a) Temperature dependencies of the raw SF and NSF neutron intensity measured at $\mathbf{Q} = (0, 1, 1)$ in sample C. (b) Sketch of the scattering plane showing the three polarization directions discussed here; $\mathbf{P} \parallel z$ corresponds to the direction perpendicular to the scattering plane (here a^*). (c) Temperature dependencies of the normalized magnetic intensity, I_{mag}, measured at $\mathbf{Q} = (0, 1, 1)$ for $\mathbf{P} \parallel \mathbf{Q}$ for the 4 underdoped samples A–D and the overdoped sample E (solid points). I_{mag} is defined as $I_{\mathrm{mag}}(T) = \alpha I_{\mathrm{NSF}}(300\ \mathrm{K})[\frac{I_{\mathrm{SF}}}{I_{\mathrm{NSF}}}(T) - \frac{I_{\mathrm{SF}}}{I_{\mathrm{NSF}}}(T \sim 300\ \mathrm{K})]$, where I_{mag} is arbitrarily set to zero in the high temperature range (~ room temperature) and $\alpha = 7/I_{004}^{\mathrm{meas}}(300\ \mathrm{K})$ calibrates the magnetic cross sections in mb using the nuclear Bragg cross section at $\mathbf{Q} = (0, 0, 4)$, $I_{004}^{\mathrm{calc}} = 7$ b. The normalized magnetic intensity for the Bragg peak, $\mathbf{Q} = (0, 0, 2)$, is also shown for samples A and C (open points). (d) Temperature dependencies of the normalized magnetic intensity measured at $\mathbf{Q} = (0, 1, 1)$ (solid points), as well as $\mathbf{Q} = (0, 0, 2)$ (open points) for $\mathbf{P} \parallel \mathbf{z}$. (e) Temperature dependencies of the normalized magnetic intensity, I_{mag}, measured at $\mathbf{Q} = (0, 1, 1)$ for sample B for $\mathbf{P} \perp \mathbf{Q}$.

shown in Figs. 1(c)–1(e) for sample B, unambiguously demonstrates the magnetic origin of the low temperature signal. More precisely, in the $\mathbf{P} \parallel \mathbf{z}$ configuration, only magnetic moments within the horizontal scattering plane but still perpendicular to $\mathbf{Q}$ are observed in the SF channel [19,20,22,23]. For $\mathbf{Q} = (0, 1, 1)$, this means that we mostly probe the magnetic moments parallel to the c^* axis. In the four underdoped samples, we observe a similar onset of the magnetic order below T_{mag} for $\mathbf{P} \parallel \mathbf{z}$ [Fig. 1(d)]. This demonstrates that the deduced magnetic moment has a well-defined component perpendicular to the CuO_2 plane, as expected. However, a closer comparison with both polarizations reveals that their intensities do not simply match. This underlines the fact that the magnetic moment also exhibits an in-plane component (within the CuO_2 plane) as the cross section in Fig. 1(c) is larger than the one in Fig. 1(d). Combining all measured polarizations in the different samples, one can then estimate a mean angle between the direction of the moments (assumed to be colinear) and the c^* axis to be $\phi = 45° \pm 20°$, valid for all samples. This value could be smaller for models with noncollinear moments.

As shown in Fig. 1(c), the typical cross section of the magnetic order is $\sim$1–2 mbarns, i.e., $\sim 10^{-4}$ of the strongest Bragg peaks. This explains why such a magnetic order was not reported before with unpolarized neutron diffraction. Because of these experimental limitations, we do not perform a detailed and quantitative determination of magnetic structure for which further work is needed. However, some qualitative aspects can be briefly discussed. First, we perform a scan along the L direction in the SF channel across the Bragg peak [Fig. 2(a)] where the difference in temperature between $T = 75$ and 275 K has been taken to remove the effect of the polarization leakage. The observed magnetic peak is resolution limited, showing that the magnetic order is characterized by long range 3D correlations at $T = 75$ K. Second, by looking at other Bragg peaks along c^* [Fig. 2(b)], we found that the magnetic intensity

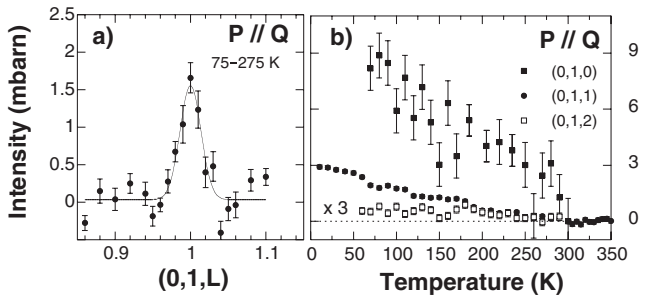

FIG. 2. (a) L-scan magnetic intensity across $Q = (0, 1, L)$ in sample A; it has been obtained using the following relation of measured quantities: $[I(\mathrm{SF}, 75\ \mathrm{K}) - I(\mathrm{SF}, 275\ \mathrm{K}) \frac{I(\mathrm{NSF},75\ \mathrm{K})}{I(\mathrm{NSF},275\ \mathrm{K})}]$ calibrated by α (see caption to Fig. 1). (b) Temperature dependencies of the magnetic intensity, I_{mag}, for various Bragg peaks $L = 0, 1, 2$ in sample A.

is not uniformly distributed versus L, meaning that (i) the magnetic intensity does not arise from the Cu-O chains, and (ii) the moments arrangement within a bilayer appears to be mainly parallel. This directly arises from the hierarchy of the observed magnetic intensities [intensity at $L = 0$ is larger than at $L = 2$, Fig. 2(b)]. Finally, using the observed magnetic cross section [Fig. 1(c)] and a weakly momentum dependent magnetic form factor, one can deduce a typical magnitude of ordered magnetic moment of $M \simeq 0.05$ to $0.1\mu_B$ with the moment decreasing with increasing doping in the four samples.

Therefore, we observe an unusual magnetic order in a temperature and doping range that cover the range where the pseudogap occurs in YBCO. Our data do not contradict previous unsuccessful polarized neutron reports [20] as the Bragg spots where the effect is observed are along a direction at 45° from the one previously studied [25]. The deduced T_{mag}, defined as the change of slope in the normalized intensity I_{mag}, decreases with increasing doping (see Table I). It scales with the pseudogap temperature, T_ρ^*, of the resistivity data in YBCO [6] as shown on Fig. 3 but does not strictly correspond to T_ρ^*. This is not surprising as the estimation of T^* from different techniques does not exactly match each other. The occurrence of a magnetic order in this temperature and doping ranges points towards a magnetic signature of an hidden order parameter associated with the pseudogap state. As all anomalous physical properties which are probing the pseudogap, the temperature dependence of the magnetic order does not exhibit a marked change at T_{mag}.

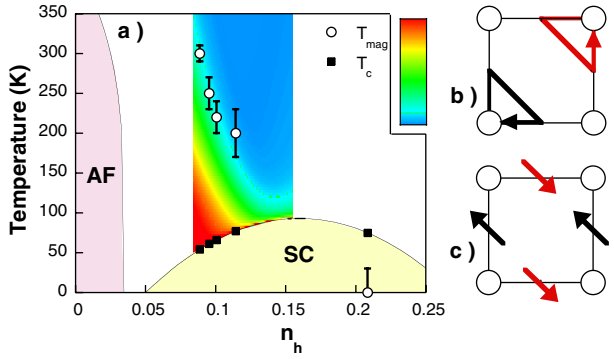

FIG. 3 (color online). (a) Cuprate superconductors phase diagram as a function of hole doping, n_h, deduced from the SC temperature using the empirical relation $T_C/T_C^{\max} = 1–82.6(n_h - 0.16)^2$ [29]. The white points show T_{mag} (see Table I). The color map shows the quantity $\delta R(T) = 1 - [\rho_{ab}(T) - \rho_{ab}(0)]/(\alpha T)$ deduced from the resistivity measurements in YBCO [6]: the change of colors indicates the departure from the T-linear behavior, $\delta R(T) = 0$ represented in blue or dark gray, at high temperature. $\delta R(T) \neq 0$ defines the pseudogap state. AF stands for antiferromagnetism. (b) Circulating current phase, Θ_{II}, in the CuO_2 plane proposed to explain the pseudogap phase in high-T_C superconducting cuprates [11,12]. (c) A spin model preserving TSL.

Being on top of nuclear Bragg peaks, that magnetic order does not break TSL, indicating a zero magnetic propagation wave vector, $\mathbf{Q} = 0$. As shown in Fig. 1(c), no magnetic intensity occurs below T_{mag} at the Bragg peak $\mathbf{Q} = (0, 0, 2)$, ruling out a ferromagnetic order. The absence of breaking of TSL points towards a magnetic pattern of antiparallel magnetic moments within each unit cell. Among the proposed order parameters, only one gives magnetic scattering at $\mathbf{Q} = (10L)[\equiv (01L)]$: it is the orbital moments arising from the circulating current phase with 2 current loops per CuO_2 unit cell, Θ_{II} [Fig. 3(b)] [11,12]. Another possibility could be a model with colinear spin moments located at the oxygen site ferromagnetic along both directions of the square lattice but antiparallel to each other as sketched in Fig. 3(c). Any other model characterized by a decoration of the CuO_2 plaquette would also give rise to a magnetic contribution at the proper Bragg spots. From our present measurements, one cannot distinguish between these two models. Only a detailed study of magnetic form factors would allow one to differentiate the scattering from spin and orbital moments.

An additional puzzling issue is why this magnetic order has not been clearly identified by local probes and, in particular, by the muon spin resonance technique. Looking at the specific pattern of the observed moments, one sees that they tend to compensate each other, likely resulting in weak dipolar magnetic fields at the muon site. In the proposed orbital model [11,12], a full cancellation even occurs for symmetric sites, such as the Cu and oxygen sites, yielding the absence of a measured effect using nuclear magnetic resonance techniques. It is also worth mentioning that the observed magnetic order is static at the neutron time scale (10^{-11} s). At present, one cannot exclude that it would be dynamic at lower time scales.

In conclusion, we report a first signature of an unusual magnetic order in several $YBa_2Cu_3O_{6+x}$ samples matching the pseudogap behavior in underdoped cuprates (Fig. 3). Such an observation points towards the existence of a hidden order parameter for the pseudogap phase in high-T_C superconductors. Importantly, our experiment reveals that a 3D long range order does not break the translational symmetry of the lattice and implies a decoration of the unit cell with staggered spin or orbital moments. The symmetry of the observed order corresponds to the one expected in orbital moments emanating from a circulating current state [11,12]. Whatever the origin of the observed order, its pattern challenges the single band Hubbard picture commonly used to describe high-T_C cuprates. At very least, oxygen orbitals need to be included to determine the minimal effective Hamiltonian for the cuprates.

We are very grateful to C. M. Varma for invaluable encouragement, comments, and ideas on these experiments. We also thank B. Keimer, J.-M. Mignot, P. Monceau, L. Pintschovius, and L.-P. Regnault for their support.

*To whom correspondence should be addressed.
Electronic address: bourges@llb.saclay.cea.fr

[1] M. R. Norman, D. P. Pines, and C. Kallin, Adv. Phys. **54**, 715 (2005).
[2] M. R. Norman and C. Pépin, Rep. Prog. Phys. **66**, 1547 (2003).
[3] T. Timusk and B. Statt, Rep. Prog. Phys. **62**, 61 (1999).
[4] J. L. Tallon and J. W. Loram, Physica (Amsterdam) **349C**, 53 (2001).
[5] H. Alloul *et al.*, Phys. Rev. Lett. **63**, 1700 (1989).
[6] T. Ito *et al.*, Phys. Rev. Lett. **70**, 3995 (1993).
[7] J. W. Loram *et al.*, Physica (Amsterdam) **235C–240C**, 134 (1994).
[8] P. A. Lee, Physica (Amsterdam) **317C–318C**, 194 (1999).
[9] V. J. Emery and S. A. Kivelson, Nature (London) **374**, 434 (1995).
[10] J. Orenstein and A. J. Millis, Science **288**, 468 (2000).
[11] C. M. Varma, Phys. Rev. B **55**, 14 554 (1997); Phys. Rev. Lett. **83**, 3538 (1999); Phys. Rev. B **73**, 155113 (2006).
[12] M. E. Simon and C. M. Varma, Phys. Rev. Lett. **89**, 247003 (2002).
[13] S. Chakravarty *et al.*, Phys. Rev. B **63**, 094503 (2001).
[14] C. Castellani *et al.*, Phys. Rev. Lett. **75**, 4650 (1995).
[15] H. C. Chen *et al.*, Phys. Rev. Lett. **93**, 187002 (2004).
[16] D. Poilblanc, Phys. Rev. B **72**, 060508 (2005).
[17] J. Zaanen *et al.*, Philos. Mag. B **81**, 1485 (2001).
[18] F. Onufrieva and P. Pfeuty, Phys. Rev. Lett. **82**, 3136 (1999).
[19] R. M. Moon *et al.*, Phys. Rev. **181**, 920 (1969).
[20] S. H. Lee *et al.*, Phys. Rev. B **60**, 10 405 (1999); Ph. Bourges and L. P. Regnault(unpublished).
[21] A. Kaminski *et al.*, Nature (London) **416**, 610 (2002); S. Borisenko *et al.*, *ibid.* **431** (2004), published online only, 2 September 2004; A. Kaminski *et al.*, *ibid.* **431** (2004), published online only, 2 September 2004.
[22] Y. Sidis *et al.*, Phys. Rev. Lett. **86**, 4100 (2001).
[23] Magnetic neutron diffraction always measures magnetic components perpendicular to the scattering wave vector. In a polarized neutron experiment, only the magnetic components perpendicular to the neutron polarization direction contribute to the spin-flip channel [19].
[24] S. P. Bayrakci *et al.*, Phys. Rev. Lett. **94**, 157205 (2005).
[25] The Bragg magnetic peaks characteristic of the two CC states proposed by [12] differ by 45°: main Bragg peaks like $\mathbf{Q} = (11L)$ are expected for the state Θ_I and like $\mathbf{Q} = (10L)[\equiv (01L)]$ for the state Θ_{II}. In both cases, no magnetic contribution occurs on Bragg peaks like $\mathbf{Q} = (00L)$.
[26] L. Pintschovius *et al.*, Phys. Rev. Lett. **89**, 037001 (2002).
[27] V. Hinkov *et al.*, Nature (London) **430**, 650 (2004).
[28] S. Pailhès *et al.*, cond-mat/0512634.
[29] J. L Tallon *et al.*, Phys. Rev. B **51**, R12911 (1995).